日本薬学会　第134年会
2014年3月27日(木)-30日(日) 熊本市総合体育館(熊本)　28日ポスター発表(28amM-098)
Robo4 近位プロモーターの DNA メチル化の Robo4 遺伝子発現への寄与
○田中亨、AirdWC、岡田欣晃、土井健史

日本薬学会　第134年会
2014年3月27日(木)-30日(日) 熊本市総合体育館(熊本)　28日ポスター発表(28amM-158)
血管内皮細胞特異的受容体Robo4の発現抑制核酸を用いた敗血症治療の可能性
○山本奈那、酒井美貴、真鍋詩織、William Aird、山本剛史、小比賀聡、岡田欣晃、土井健史

日本薬学会　第134年会
2014年3月27日(木)-30日(日) 熊本大学黒髪キャンパス(熊本)30日口頭発表(30Y-pm13)
血管内皮細胞特異的受容体Robo4の過剰発現が炎症応答に及ぼす影響の解析
○白倉圭佑、山内沙織、William C. Aird、岡田欣晃、土井健史

日本薬学会　第134年会
2014年3月27日(木)-30日(日) 熊本大学黒髪キャンパス(熊本)30日口頭発表(30O-pm16S)
架橋型人工核酸を用いた splice-switching oligonucleotides の配列設計
○下 剛典、橘 敬祐、斎藤 究、脇 玲子、山本剛史、土井健史、小比賀 聡

H. 知的財産権の出願・登録状況(予定を含む)

なし

厚生労働科学研究費補助金
難病・がん等の疾患分野の医療の実用化研究事業（再生医療関係研究分野）
分担研究報告書

疾患特異的 iPS 由来肝細胞を用いた薬効評価

分担代表者　大阪大学薬学研究科　水口　裕之

本研究では、健常者由来 iPS 細胞、あるいは疾患特異的 iPS 細胞から作製した標的組織（心臓、血管、運動器、眼、内分泌、肝臓）を用いたスクリーニングにより、創薬開発の効率化、安全性の向上に資する基盤構築を目的としている。本研究において我々は、遺伝子異常を伴う先天性難治疾患の病態解明や疾患モデルの開発、治療薬創出に期待されている遺伝病患者から作製した iPS 細胞疾患（特異的 iPS 細胞）から肝細胞を分化誘導し、有効な疾患モデル細胞を用いた新規薬効評価系の構築を行う。本年度は、これまで有効な治療薬が開発されておらず、救命のために肝移植を要する肝臓疾患である進行性家族性胆汁うっ滞症（progressive familial intrahepatic cholestasis; PFIC）2 型患者由来の iPS 細胞の樹立を行い、肝細胞への分化誘導に着手した。

研究協力者

今川和生　(独)医薬基盤研究所
大阪大学大学院薬学研究科
筑波大学医学医療系

高山和雄　大阪大学大学院薬学研究科
(独)医薬基盤研究所

A. 研究目的

遺伝子異常を伴う先天性難治疾患の病態解明や疾患モデルの開発、治療薬創出に、遺伝病患者から作製した iPS 細胞は有効な疾患モデル細胞になると期待されている。本研究では、これまで有効な治療薬が開発されておらず、救命のために肝移植を要する肝臓疾患である PFIC2 型に焦点をあて、これらの患者由来の iPS 細胞の樹立と肝細胞への分化誘導、病態解明と治療薬創出を行う。PFIC2 型は胆汁生成や薬物排泄に関わるトランスポーターBSEP（bile salt export pump, ABCB11）に約 10 万人に 1 人の割合で遺伝子異常があり、強い黄疸や全身掻痒を来すほか、高度の胆汁うっ滞性肝障害を起こし、肝硬変、肝不全へと進展して致死的な経過を辿る。本疾患に対する疾患モデルの開発や病態解明、治療薬の創出が強く望まれている。

B. 研究方法

筑波大学医学医療系小児科学教室および独立行政法人医薬基盤研究所（研究分担者・水口が招へいプロジェクトリーダーを併任）との連携により、筑波大学附属病院及び関連施設で診療中の PFIC2 型患者、および健常人数名の末梢血から、定法に従いセンダイウイルスベクター（DNAVEC 社）を用いてインテグレーションフリーiPS 細胞を樹立した。

ヒト iPS 細胞から肝細胞への分化は、内胚葉、肝幹前駆細胞を経由して行った。内胚葉への分化過程（day 0 から day 4）には 100 ng/ml Activin A (R&D systems)を含む L-wnt3a-conditioned differentiation RPMI1640 medium を、肝幹前駆細胞への分化過程(day 4 から day 9)には 20 ng/ml FGF4（R&D system）、20 ng/ml bone morphogenetic protein 4（BMP4）(R&D systems) を含む differentiation RPMI1640 培地を、肝細胞への分化過程の前期（day 9 から day 14）には 20 ng/ml hepatocyte growth factor（HGF）（R&D systems) を含む differentiation RPMI1640 medium を、後期（day 14 から day 25）には、20 ng/mL Oncostatin M（OsM、R&D systems）を含む HCM を用いて培養した。

（倫理面への配慮）

ヒト試料を用いた研究を実施する場合には、各研究機関等で定められた倫理規定を遵守して研究を遂行した。

C. 研究結果

健常人および PFIC2 型患者から採取した末梢血から、山中 4 因子を発現するセンダイウイルスベクターを用いてインテグレーションフリーiPS 細胞を樹立した。末梢血に山中 4 因子を遺伝子導入することで、典型的な iPS 細胞様コロニーが多数出現した。また、これらのコロニーにおいて、未分化マーカーの OCT3/4 が発現していることを免疫組織染色で確認した。したがって、健常人および PFIC2 型患者由来末梢血からヒト iPS 細胞が樹立できたことが明らかとなった。

健常人および PFIC2 型患者由来 iPS 細胞の性質をさらに詳細に評価するために、未分化関連遺伝子の発現を解析した。その結果、樹立した iPS 細胞株における未分化関連遺伝子の発現量は当研究室で従来培養しているヒト ES 細胞やヒト iPS 細胞と同程度であることを確認した。

次に、樹立した iPS 細胞株の肝分化能をの検討を行った。その結果、樹立した iPS 細胞株はアルブミン産生能をもつ肝細胞に分化できることが確認できた。次年度以降、より詳細な肝細胞機能について検討予定である。

D. 考察

重篤な病態を示し、医療上の必要性が高

いにも関わらず、患者数が少ないこともあり、これまで全く治療法がなかった希少疾患に対する治療薬の開発研究に対する支援は、厚生労働行政上、極めて大きな期待がかけられている。本研究で治療法開発を検討するPFIC2型は、これまで有効な治療薬は開発されておらず、重篤な肝障害からしばしば死に至る疾病であり、肝移植のみが唯一の有効な治療法である。また、例えば、PFIC2型の原因遺伝子であるBSEP遺伝子をノックアウトしたマウスでは、ヒトの場合とは異なりBSEP以外の胆汁酸トランスポーターが胆汁酸排泄を補完することから黄疸や肝障害は軽度示すのみであり、これまで疾患解析には用いられなかった。そこで本研究では、iPS細胞技術と肝細胞への高効率分化誘導技術を駆使して、PFIC2型の疾患モデル細胞を作製し、新規疾患モデルの開発や病態解明、さらには治療薬の創出までを目指す。iPS細胞技術を利用した本研究のような研究手法により、従来は移植による治療法しか存在しなかった疾患に対する新規治療法が開発できれば、医療経済的にも有益である。これらは、国民の健康の増進に資するものであり、厚生労働行政上、極めて意義深い。

E. 結論

健常人およびPFIC2型患者から採取した末梢血からiPS細胞を作製し、肝細胞分化研究に着手した。次年度は、本iPS細胞から分化誘導した肝細胞の機能を詳細に検討予定である。

F. 研究発表

1. 論文発表

1) Takayama K., Nagamoto Y., Mimura N., Tashiro K., Sakurai F., Tachibana M., Hayakawa T., Kawabata K., Mizuguchi H. Long-term self-renewal of human ES/iPS-derived hepatoblast-like cells on human Laminin 111-coated dishes. *Stem Cell Rep.*, 1, 322-335 (2013)

2) Takayama K., Kawabata K., Nagamoto Y., Inamura M., Ohashi K., Okuno H., Yamaguchi T., Tashiro K., Sakurai F., Hayakawa T., Okano T., Furue MK., Mizuguchi H. CCAAT/enhancer binding protein-mediated regulation of TGFβ receptor 2 expression determine the hepatoblast fate decision. *Development*, 141, 91-100 (2014)

3) Watanabe H., Takayama K., Inamura M., Tachibana M., Mimura N., Tashiro K., Nagamoto Y., Sakurai F., Kawabata K., Furue MK., Mizuguchi H. HEX Promotes Hepatic-Lineage Specification Through the Negative Regulation of Eomesodermin. *PLoS ONE*, 9, e90791 (2014)

4) Nagamoto Y., Takayama K., Tashiro K., Tateno C., Sakurai F., Tachibana M., Kawabata K., Ikeda K., Tanaka Y., Mizuguchi H. Efficient engraftment of human iPS cell-derived hepatocyte-like cells in uPA/SCID mice by overexpression of FNK, a Bcl-xL mutant gene. *Cell Transplantation*, in press.

2. 学会発表

1) Takayama K., Nagamoto Y., Kawabata K., Tashiro K., Sakurai F., Tachibana M., Mizuguchi H. Long-term culture of hepatoblast-like cells derived from human pluripotent stem cells, Boston, June, 2013

2) Nagamoto Y., Takayama K., Tashiro K., Tateno C., Sakurai F., Tachibana F., Kawabata K., Ikeda K., Tanaka Y., Mizuguchi H. Comparative analysis of transplantation efficacy of human iPS cell-derived hepatic cells at various differentiation stages in mice. International Society for Stem Cell Research 11th Annual Meeting, Boston, June, 2013

3) Takayama K., Nagamoto Y., Tashiro K., Sakurai F., Tachibana M., Kawabata K., Mizuguchi H. Long-term culture of hepatoblast-like cells derived from human ES/iPS cells、第 20 回大会、肝細胞研究会、大阪、2013 年 9 月

4) Nagamoto Y., Takayama K., Tashiro K., Tateno C., Sakurai F., Tachibana F., Kawabata K., Ikeda K., Tanaka Y., Mizuguchi H. Over-expression of Bcl-xL mutant (FNK) improves the engraftment efficacy of human iPS cell-derived hepatocytes in the liver of uPA/SCID mice、第 20 回大会、肝細胞研究会、大阪、2013 年 9 月

5) Takayama K., Morisaki Y., Furukawa N., Higuchi M., Ohtaka M., Nishimura K., Nakanishi M., Tachibana M., Sakurai F., Kawabata K., Mizuguchi H. Comparison of Hepatic Functions Between Genetically Identical Primary Human Hepatocytes and Human iPS-Derived Hepatocyte-Like Cells、第 28 回日本薬物動態学会年会、東京、2013 年 10 月

6) 高山和雄、長基康人、田代克久、櫻井文教、立花雅史、川端健二、水口裕之、ヒト多能性幹細胞から分化誘導した肝幹・前駆細胞の維持と複製、第 36 回日本分子生物学会、神戸、2013 年 12 月

7) Takayama K., Nagamoto Y., Tashiro K., Sakurai F., Tachibana M., Kawabata K., Mizuguchi H. Generation of long-term expandable hepatoblasts differentiated from human iPS cells

enables large-scale preparation of hepatocytes for drug discovery and development. The 7th Takeda Science Foundation Symposium on PharmaSciences (iPS Cells in Drug Discovery & Development)、大阪、2014年1月

8) 長基康人、高山和雄、田代克久、立野知世、櫻井文教、立花雅史、川端健二、池田一雄、田中靖人、水口裕之、活性型Bcl-xL (FNK) 過剰発現によるヒト iPS細胞由来肝細胞のマウス生着効率向上、京都、第13回再生医療学会総会、2014年3月

9) 長基康人、高山和雄、田代克久、立野知世、櫻井文教、立花雅史、川端健二、池田一雄、田中靖人、水口裕之、活性増強型Bcl-xL (FNK) 過剰発現を利用したヒト iPS 細胞由来肝細胞のマウス肝置換効率向上、熊本、日本薬学会第134年会、2014年3月

10) 岡本涼太、長基康人、高山和雄、大橋一夫、櫻井文教、立花雅史、川端健二、水口裕之、ヒトiPS細胞由来肝細胞の腎被膜下への移植、熊本、日本薬学会第134年会、2014年3月

G. 知的財産権の出願・登録状況

1. 特許取得

該当無し

2. 実用新案登録

該当無し

3. その他

該当無し

厚生労働科学研究費補助金
難病・がん等の疾患分野の医療の実用化研究事業（再生医療関係研究分野）
分担研究報告書

組織構築に関する研究

研究分担者　大阪大学工学研究科　明石　満

研究要旨
iPS 細胞由来心筋細胞を用いる予備実験として、ラット新生仔心筋細胞を単離し、三次元組織構築を試みた。心筋細胞表面にフィブロネクチンとゼラチンのナノ薄膜を交互積層法により構築し、セルカルチャーインサートに播種・培養することで、およそ 3-4 日後に組織全体が拍動する三次元組織体が得られた。播種細胞数に依存し、およそ 10 層の組織体を構築可能であった。また、拍動数を増加させる効果があるイソプロテレノールの添加によって拍動数の増加が確認された。得られた三次元心筋組織体は、創薬分野への応用が期待される。

A．研究目的

iPS 細胞由来心筋細胞を用いる予備実験として、ラット新生仔心筋細胞を単離し、三次元組織構築を試みた。また、心筋細胞の三次元構築の最適条件を検証し、得られた組織体の薬剤応答性を評価した。iPS 細胞由来心筋細胞の組織構築の最適条件も検証した。

B．研究方法

単離した心筋細胞を 0.2 mg/ml のフィブロネクチン／50 mM トリス緩衝液と 0.2 mg/ml のゼラチン／50 mM トリス緩衝液に各 1 分間ずつ浸漬し、合計で 9 回交互浸漬を行った。得られた $1x10^6$ 個の細胞をセルカルチャーインサートへ播種し、所定時間培養した。得られた組織体の拍動数を位相差顕微鏡よりカウントした。さらに、1 μM のイソプロテレノール 100 μl を培地に添加し、30 分インキュベート後の拍動数をカウントした。

iPS 細胞由来心筋細胞の純化法を検証し、心筋細胞の純度による、iPS 細胞由来心筋組織の電気生理学的特性の変化を検討した。

（倫理面への配慮）

本研究における動物実験は、大阪大学動物実験施設、およびその管理下にある別施設にて行い、すべて「動物の愛護及び管理に関する法律」、「実験動物の飼養及び保管並びに苦痛の軽減に関する基準」を遵守しておこなった。すべての動物実験は、各施設の動物実験の倫理性、妥当性に関する審査委員会の承認を得た実験計画書にもとづき、これを遵守しておこなった。

C．研究結果

1．心筋組織の構築方法の確立

現在 iPS 細胞から心筋細胞への分化誘導に成功している（図 1）。また、iPS 細胞由来心筋細胞の組織化の前に、新生仔心筋細胞を用いた三次組織体を構築し（図 2）、播種細胞数に依存して最大 10 層の組織体の構築が確認された。拍動数はおよそ 4 日後に最大となり、その後は培養期間に伴い減

少する結果となった。また、層数に依存して拍動数が増加する傾向が得られた。イソプロテレノールを添加することで、53回／1分間の拍動数が84回／1分間に増加した（図3）。新生仔心筋細胞組織の組織体は構築可能となったため、iPS 細胞由来心筋細胞の組織体の作成に着手し、同組織は、同調した拍動を示す三次元心筋組織であった（図4）。またこれまでの三次元構築法を用いて作成した心筋組織は組織体に空隙がるため、心筋細胞の組織化に関して、新しい方法論の確立が必要である。これまでの積層化法は18回の遠心分離を行うため、細胞のバイアビリティーが低下してしまうが、セルカルチャーインサートのポアを利用したフィルター法を使用した場合、細胞のダメージが少なく、組織構築も可能であることが判明した。

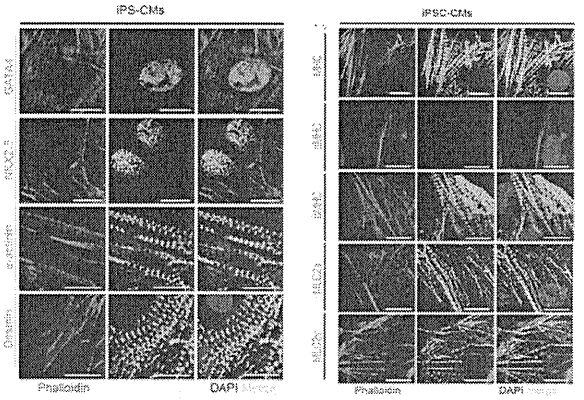

図1．iPS 細胞由来心筋細胞

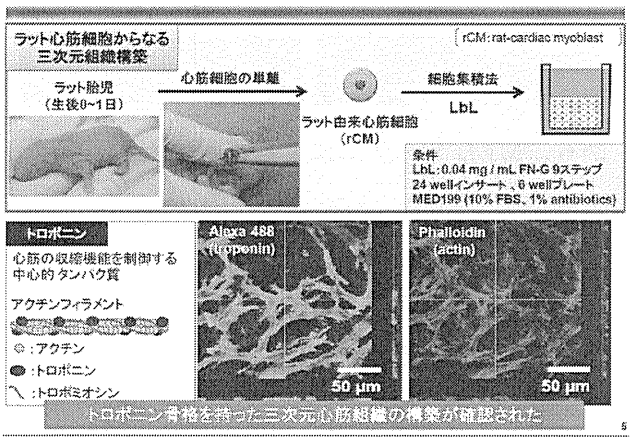

図2．新生仔心筋細胞を用いた三次組織体の構築

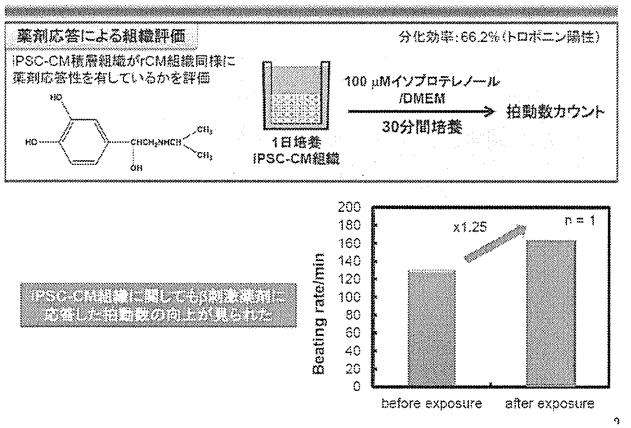

図3．iPS 積層組織に対する薬剤応答性の評価

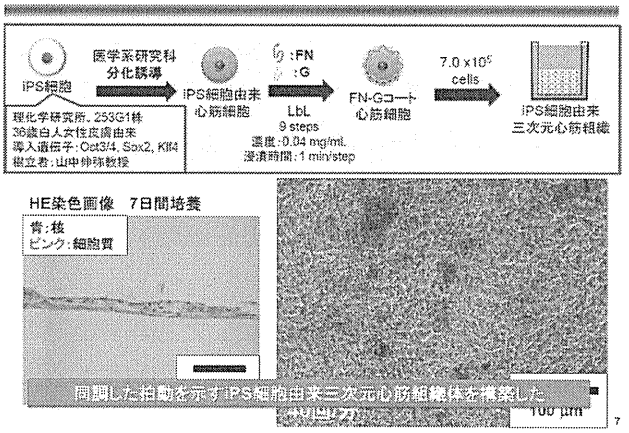

図4．iPS 細胞由来三次元心筋組織

2．iPS 細胞由来心筋細胞の純化技術の開発、電気生理学的検討

iPS 細胞からの心筋分化誘導方法については、様々な方法が報告されているが、90%を超える純度の細胞を安定して得ることは困難である。さらに、生体の心筋組織においては、心筋細胞の割合は半分以下とされており、必ずしも高純度の心筋細胞を用いることが生体の反応を反映しているとは限らない。そこで、本研究では、まず、iPS 細胞から心筋分化誘導を行った細胞集団から心筋細胞を精製する方法について検討した。さらに、より生体に近い心筋細胞組織を形成するため、様々な心筋細胞純度の組織体を形成し、その機能の違いについて比較評価を行った。

心筋細胞の精製法として、細胞表面マーカーを用いた MACS 磁気細胞分離法による分離精製を検討した。さらに、MACS により分離した心筋細胞を用いて心筋細胞純度 25、50、70、90%の細

胞組織体を形成し、シート形成、電気伝導速度等の比較解析を行った。

多能性幹細胞から分化誘導した心筋細胞において発現している表面マーカーとして、CD106, CD166, CD172 が報告されている。そこで、我々の分化誘導法により分化させた心筋細胞において、これらのマーカーを用いて心筋細胞を分離することが可能か否かを検討した。

CD106、CD166、CD172 と心筋細胞マーカーであるトロポニン T との 2 重染色を行ったところ、CD106、CD172 が TnT との高い相関を示した。次に、CD106、CD172 に対する抗体を用いて MACS 磁気細胞分離を行ったところ、それぞれの陽性分画には純度約 90%の心筋細胞を精製することが可能であった(図 5)。

MACS 磁気分離によって生成した心筋細胞を用いて各純度に調整した細胞を播種し、MED システムにより細胞外電位を測定した。その結果、いずれの純度でも 3 日目には一部電位が検出されない測定チャネルが存在したが、50%以上の場合には 5 日目には全体で同期的な電位が検出された。一方、純度 25%の場合には、5 日目でも電位が検出されない測定チャネルが存在した（図 6）。

細胞外電位のデータから、電位の伝導速度を算出したところ、心筋細胞純度が高いほど伝導速度が速い傾向がみられた（図 7）。

D．考察

研究者らのオリジナルの組織構築法、細胞集積法を用いることで、ラット新生仔由来心筋細胞の三次元組織体の構築が可能であった。得られた組織体は薬剤に応答して拍動数が増加する結果となり、創薬分野への応用が期待される。次年度はヒト iPS 細胞由来心筋細胞を用いて、電気生理学的、組織学的に心筋組織と相同性が高い三次元組織体の構築に取り組む予定である。

E．結論

本プロジェクトで作成した各種心筋組織体を用いて新規低分子ライブラリーの心毒性、各種有効性を ex vivo で示すことにより、ドラッグリポジショニング、新規薬剤の開発が可能であるものと思われる。

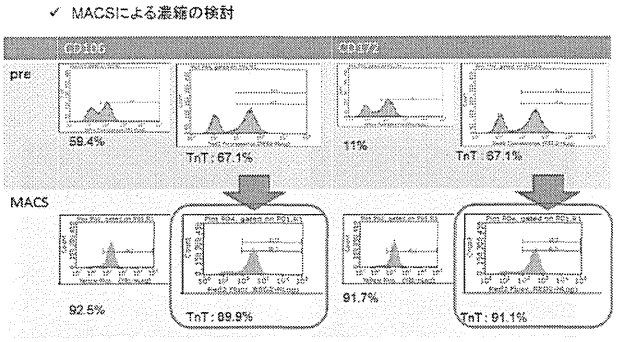

図 5．心筋精製法の検討

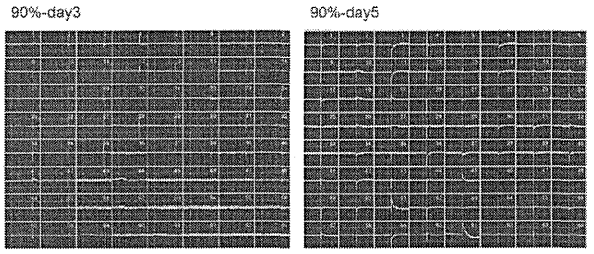

図 6．MED システムによる細胞外電位測定

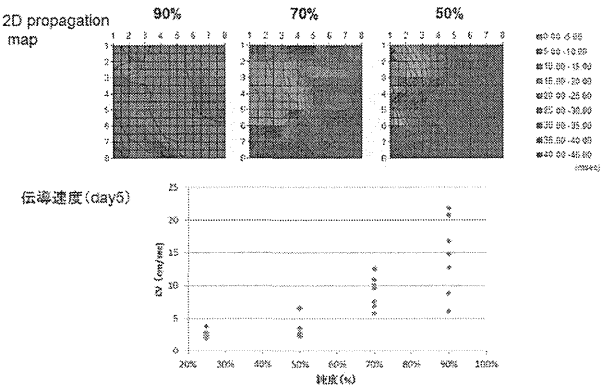

図 7．細胞外電位の伝播パターン

F．健康危険情報

報告なし。

G．研究発表

1．論文発表

２．学会発表

天野雄斗・西口昭広・松崎典弥・宮川繁・澤芳樹・明石満

「細胞集積法を用いたiPS細胞由来の正常・疾患特異的三次元心筋モデルの構築とその薬剤評価への応用」

文部科学省主催　第３回サイエンス・インカレ

2014年３月１日

H．知的財産権の出願・登録状況(予定を含む)

１．特許取得

出願番号：特願2013-173745

発明者：明石　満・松崎典弥・澤　芳樹・宮川　繁

発明の名称：薬剤候補化合物のスクリーニングに用いる心筋組織チップの製造方法

出願人：国立大学法人大阪大学

出願日：2013年８月23日

２．実用新案登録

３．その他

別紙４

研究成果の刊行に関する一覧表レイアウト（参考）

雑誌

発表者氏名	論文タイトル名	発表誌名	巻号	ページ	出版年
Yasuhiro Shudo, Shigeru Miyagawa, Hanayuki Ohkura, Satsuki Fukushima, Atsuhiro Saito, Motoko Shiozaki, Naomasa Kawaguchi, Nariaki Matsuura, Tatsuya Shimizu, Teruo Okano, Akifumi Matsuyama, and Yoshiki Sawa	Addition of Mesenchymal Stem Cells Enhances the Therapeutic Effects of Skeletal Myoblast Cell-Sheet Transplantation in a Rat Ischemic Cardiomyopathy Model	TISSUE ENGINEERING	Part A,Vol.20	728-739	2014
Yu T, Miyagawa S, Miki K, Saito A, Fukushima S, Higuchi T, Kawamura, Kawamura T, Ito E, Kawaguchi N, Sawa Y, Matsuura N.	In vivo differentiation of induced pluripotent stem cell-derived cardiomyocytes	Circ J	77(5)	1297-306	2013
Kawamura M, Miyagawa S, Fukushima S, Saito A, Miki K, Ito E, Sougawa N,Kawamura T, Daimon T, Shimizu T, Okano T, Toda K, Sawa Y.	Enhanced survival of transplanted human induced pluripotent stem cell-derived cardiomyocytes by the combination of cell sheets with the pedicled omental flap technique in a porcine heart	Circulation	128(11 Suppl 1)	S87-94	2013
Outani, H., Okada, M., Yamashita, A., Nakagawa, K., Yoshikawa, H., Tsumaki, N.	Direct induction of chondrogenic cells from human dermal fibroblast culture by defined factors.	PLoS ONE	8	e77365	2013
Honda, H., Tamai, N., Naka, N., Yoshikawa, H., Myoui, A.	Bone tissue engineering with bone marrow-derived stromal cells integrated with concentrated growth factor in Rattus norvegicus calvaria defect model.	Journal of Artificial Organs	16	305-315	2013
Fujiwara M, Namba N, Miura K, Kitaoka T, Hirai H, Kondou H, Shimotsuji T, Numakura C, Ozono K.	Detection and Characterization of Two Novel Mutations in the HNF4A Gene in Maturity-Onset Diabetes of the Young Type 1 in Two Japanese Families	Horm Res Paediatr	79(4)	220-226	2013

Ichimori H, Kogaki S, Takahashi K, Ishida H, Narita J, Nawa N, Baden H, Uchikawa T, Okada Y, Ozono K.	Drastic shift from positive to negative estrogen effect on bone morphogenetic protein signaling in pulmonary arterial endothelial cells under hypoxia.	Circ J	77 (8)	2118-2126	2013
Robinson JW, Dickey DM, Miura K, Michigami T, Ozono K, Potter LR	A human skeletal overgrowth mutation increases maximal velocity and blocks desensitization of guanylyl cyclase-B	Bone	56 (2)	375-382	2013
Yoshinori Oie and Kohji Nishida	Regenerative Medicine for the Cornea	BioMed Research International	Volume 2013,	Article ID 428247	2013
Dong Shi, Yoshimasa Takano, Toru Nakazawa, MinGe Mengkegale, Shunji Yokokura, Kohji Nishida, Nobuo Fuse	Molecular genetic analysis of primary open-angle glaucoma, normal tension glaucoma, and developmental glaucoma for the VAV2 and VAV3 gene variants in Japanese subjects	Biochemical and Biophysical Research Communications	432	509-512	2013
Yingli Li, Tomoyuki Inoue, Fumihiko Takamatsu, Naoyuki Maeda, Yuichi Ohashi, and Kohji Nishida	Development of Genetically Modified Eliminable Human Dermal Fibroblast Feeder Cells for Ocular Surface Regeneration Medicine	Invest Ophthalmol Vis Sci.	54	7523	2013
Toyoshige Kobayashi, Kazutoshi Kan, Kohji Nishida, Masayuki Yamato,Teruo Okano	Corneal regeneration by transplantation of corneal epithelial cell sheets fabricated with automated cell culture system in rabbit model	Biomaterials	34	9010-9017	2013
Dong Shi, Tomoyo Funayama, Yukihiko Mashima, Yoshimasa Takano, Ai Shimizu, Kotaro Yamamoto, MinGe Mengkegale, Akiko Miyazawa, Noriko Yasuda, Takeo Fukuchi,Haruki Abe, Hidenao Ideta, Kohji Nishida, Toru Nakazawa, Julia E. Richards, Nobuo Fuse	Association of HK2 and NCK2 with Normal Tension Glaucoma in the Japanese Population	PLOS ONE	8	e54115	2013

Yoshida T, Yoshioka Y, Tochigi S, Hirai T, Uji M, Ichihashi K, Nagano K, Abe Y, Kamada H, Tsunoda S, Nabeshi H, Higashisaka K, Yoshikawa T, Tsutsumi Y.	Intranasal exposure to amorphous nanosilica particles could activate intrinsic coagulation cascade and platelets in mice.	Part Fibre Toxicol.	10	41	2013
Okada Y, Watanabe M, Nakai T, Kamikawa Y, Shimizu M, Fukuhara Y, Yonekura M, Matsuura E, Hoshika Y, Nagai R, Aird WC, Doi T.,	RUNX1, but not its familial platelet disorder mutants, synergistically activates PF4 gene expression in combination with ETS family proteins.	J.Thromb. Haemost.	11	1742-1750	2013
Tachibana K, Takeuchi K, Inada H, Sugimoto K, Ishimoto K, Yamashita M, Maegawa T, Yamasaki D, Osada S, Tanaka T, Rakugi H, Hamakubo T, Sakai J, Kodama	Human mannose-binding lectin 2 is directly regulated by peroxisome proliferator-activated receptors via a peroxisome proliferator responsive element.	J. Biochem.	154	265-273	2013
Takayama K., Nagamoto Y., Mimura N., Tashiro K., Sakurai F., Tachibana M., Hayakawa T., Kawabata K., Mizuguchi H.	Long-term self-renewal of human ES/iPS-derived hepatoblast-like cells on human Laminin 111-coated dishes.	Stem Cell Rep.	1	322-335	2013
Takayama K., Kawabata K., Nagamoto Y., Inamura M., Ohashi K., Okuno H., Yamaguchi T., Tashiro K., Sakurai F., Hayakawa T., Okano T., Furue MK., Mizuguchi H.	CCAAT/enhancer binding protein-mediated regulation of TGFß receptor 2 expression determine the hepatoblast fate decision.	Development	141	91-100	2014
Watanabe H., Takayama K., Inamura M., Tachibana M., Mimura N., Tashiro K., Nagamoto Y., Sakurai F., Kawabata K., Furue MK., Mizuguchi H.	HHEX Promotes Hepatic-Lineage Specification Through the Negative Regulation of Eomesodermin.	PLoS ONE	9	e90791	2014
Nagamoto Y., Takayama K., Tashiro K., Tateno C., Sakurai F., Tachibana M., Kawabata K., Ikeda K., Tanaka Y., Mizuguchi H.	Efficient engraftment of human iPS cell-derived hepatocyte-like cells in uPA/SCID mice by overexpression of FNK, a Bcl-xL mutant gene.	Cell Transplantation	in press	in press	in press

TISSUE ENGINEERING: Part A
Volume 20, Numbers 3 and 4, 2014

DOI: 10.1089/ten.tea.2012.0534

Addition of Mesenchymal Stem Cells Enhances the Therapeutic Effects of Skeletal Myoblast Cell-Sheet Transplantation in a Rat Ischemic Cardiomyopathy Model

Yasuhiro Shudo, MD,[1] Shigeru Miyagawa, MD, PhD,[1] Hanayuki Ohkura, PhD,[1,2] Satsuki Fukushima, MD, PhD,[1] Atsuhiro Saito, PhD,[1] Motoko Shiozaki, PhD,[1] Naomasa Kawaguchi, PhD,[3] Nariaki Matsuura, MD, PhD,[3] Tatsuya Shimizu, MD, PhD,[4] Teruo Okano, PhD,[4] Akifumi Matsuyama, MD, PhD,[2] and Yoshiki Sawa, MD, PhD[1]

Introduction: Functional skeletal myoblasts (SMBs) are transplanted into the heart effectively and safely as cell sheets, which induce functional recovery in myocardial infarction (MI) patients without lethal arrhythmia. However, their therapeutic effect is limited by ischemia. Mesenchymal stem cells (MSCs) have prosurvival/proliferation and antiapoptotic effects on co-cultured cells *in vitro*. We hypothesized that adding MSCs to the SMB cell sheets might enhance SMB survival post-transplantation and improve their therapeutic effects.
Methods and Results: Cell sheets of primary SMBs of male Lewis rats (r-SMBs), primary MSCs of human female fat tissues (h-MSCs), and their co-cultures were generated using temperature-responsive dishes. The levels of candidate paracrine factors, rat hepatocyte growth factor and vascular endothelial growth factor, *in vitro* were significantly greater in the h-MSC/r-SMB co-cultures than in those containing r-SMBs only, by real-time PCR and enzyme-linked immunosorbent assay (ELISA). MI was generated by left-coronary artery occlusion in female athymic nude rats. Two weeks later, co-cultured r-SMB or h-MSC cell sheets were implanted or no treatment was performed ($n=10$ each). Eight weeks later, systolic and diastolic function parameters were improved in all three treatment groups compared to no treatment, with the greatest improvement in the co-cultured cell sheet transplantation group. Consistent results were found for capillary density, collagen accumulation, myocyte hypertrophy, Akt-signaling, STAT3 signaling, and survival of transplanted cells of rat origin, and were related to poly (ADP-ribose) polymerase-dependent signal transduction.
Conclusions: Adding MSCs to SMB cell sheets enhanced the sheets' angiogenesis-related paracrine mechanics and, consequently, functional recovery in a rat MI model, suggesting a possible strategy for clinical applications.

Introduction

A RECENT LARGE-SCALE clinical trial, in which autologous skeletal myoblasts (SMBs) were directly injected into the heart by needle, reported only modest therapeutic benefits and a substantial risk of ventricular arrhythmias, due at least partly to the delivery method.[1,2] The major drawbacks of SMB delivery by needle injection are poor cell survival in the heart, leading to insufficient paracrine effects, and mechanical myocardial injury, potentially causing lethal arrhythmia.[1–3] In contrast, cell-sheet techniques, which we developed, deliver SMBs more effectively with minimal myocardial injury, enhanced paracrine effects, and consequently better cardiac function than attained by needle injection.[4–8]

The mechanism by which damaged myocardium is restored by transplanted SMB cell sheets is complex, involving many pathways.[4–8] Recent reports show beneficial effects of SMB cell-sheet transplantation in several animal experimental models and patients with heart failure, which are primarily attributed to cytokine secretion from the transplanted cell sheets (i.e., a paracrine effect).[4–9]

However, SMB cell sheets attached to the surface of the infarcted myocardium are poorly supported by the vascular

Presented at the American Heart Association, Orlando, Florida, November 12–15, 2011.
[1]Department of Cardiovascular Surgery, Osaka University Graduate School of Medicine, Suita, Japan.
[2]Laboratory for Somatic Stem Cell Therapy, Foundation of Biomedical Research and Innovation, Kobe, Japan.
[3]Department of Pathology, Osaka University Graduate School of Medicine, Suita, Japan.
[4]Institute of Advanced Biomedical Engineering and Science, Tokyo Women's Medical University, Tokyo, Japan.

network of the native myocardium, which limits the survival of the SMBs and, consequently, their therapeutic effects.[7] Thus, conventional SMB cell-sheet transplantation might be insufficient to repair severely damaged myocardium, which has poor viability. Mesenchymal stem cells (MSCs) are used as feeder cells to support the survival, proliferation, and differentiation of co-cultured stem/progenitor cells *in vitro*.[10–12] Moreover, MSCs are advantageous for cellular therapy because they are multipotent, potentially immune privileged, and expand easily *ex vivo*. MSCs also proliferate rapidly and induce angiogenesis.[13,14]

We hypothesized that adding MSCs to the SMB cell sheets *in vitro* might enhance their survival and function after transplantation, which might enhance the benefits of SMB cell-sheet transplantation therapy. Here, we investigated whether co-culturing SMBs with MSCs would enhance the SMBs' cytokine production *in vitro*. We also examined the therapeutic effects on chronic ischemic heart failure of transplanting cell sheets created from co-cultured SMBs and MSCs, compared with SMB-only and MSC-only cell sheets.

Materials and Methods

This study was approved by the Institutional Ethics Committee of the Osaka University. Humane animal care was used in compliance with the "Principles of Laboratory Animal Care" formulated by the National Society for Medical Research, and the "Guide for the Care and Use of Laboratory Animals" prepared by the Institute of Animal Resources and published by the National Institutes of Health (Publication No. 85–23, revised 1996). All procedures and evaluations, including assessments of cardiac parameters, were carried out in a blinded manner. The authors had full access to the data and take full responsibility for its integrity. All authors have read and agreed to the article as written.

Isolation of SMBs and adipose tissue-derived mesenchymal cells, and cell-sheet preparation

Primary skeletal myoblasts of rat origin (r-SMBs) were isolated from Lewis rats (3 weeks old, male; CLEA Japan, Inc.) and expanded *in vitro* as described previously[7,8]: more than 70% of the isolated cells were actin positive and 60–70% were desmin positive, as determined by flow cytometry (data not shown). To detect r-SMBs, we used GFP transgenic Lewis rats.[15] Primary human MSCs (h-MSCs) were isolated from female subcutaneous adipose tissue samples as described.[12] h-MSCs exhibit mesenchymal morphology (Fig. 1A). Cell sheets consisting of r-SMBs or h-MSCs were prepared using temperature-responsive culture dishes (UpCell®; CellSeed), as described.[12] Cell sheets containing both r-SMBs and h-MSCs were prepared by co-culturing these cells in temperature-responsive culture dishes.

Rat myocardial infarction model and cell-sheet implantation

A proximal site of the left anterior descending coronary artery (LCA) of athymic nude rats (F344/NJcl-rnu/rnu, 8-week-old, female, 120–130 g; CLEA Japan) was permanently occluded using a thoracotomy approach. The animals were then kept in temperature-controlled individual cages for 2 weeks to generate a subacute ischemic heart failure model.[7,8,12] The rats were then divided into 4 experimental groups ($n=10$ in each) as follows: (1) transplantation of triple-layer h-MSC cell sheets (7.5×10^5 cells per sheet), (2) transplantation of triple-layer r-SMB cell sheets (3.0×10^6 cells per sheet), (3) transplantation of triple-layer co-cultured r-SMB (3.0×10^6 cells per sheet) and h-MSC (7.5×10^5 cells per sheet) sheets, and (4) no treatment (control) (Fig. 1B). Thereafter, the rats were kept in individual cages for 4 weeks.

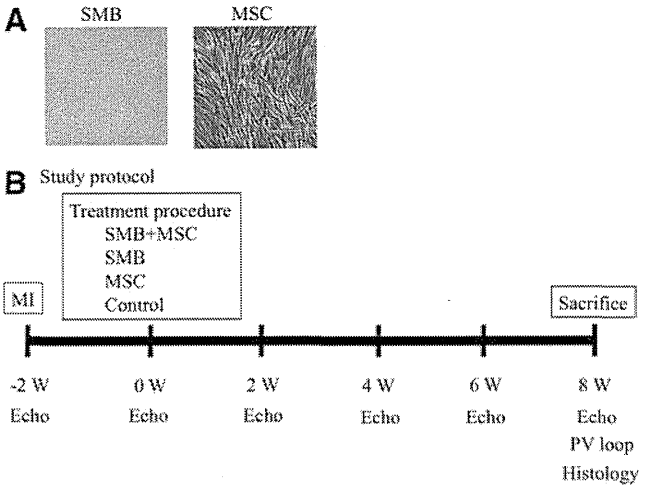

FIG. 1. **(A)** Morphology of SMB and MSC. **(B)** Study protocol used for the assessment of cardiac function and histology. Athymic nude rats (F344/NJcl-rnu/rnu) underwent induction of myocardial infarction by occluding the LAD permanently, followed by the treatment procedure 2 weeks later. Cardiac function was assessed by echocardiography just before 2, 4, 6, and 8 weeks after the treatment procedure. Eight weeks after the treatment procedure, invasive hemodynamic analysis and histological examination were performed following the sacrifice. SMB+MSC, co-culture of SMBs and MSCs; SMB, skeletal myoblast; MSC, derived mesenchymal stem cell; Echo, echocardiography; PV loop, invasive hemodynamic analysis. Color images available online at www.liebertpub.com/tea

Echocardiography

Echocardiography was performed under general anesthesia using 1% isoflurane just before, and 2, 4, 6, and 8 weeks after the treatment procedure (SONOS 7500; Philips Medical Systems) (Fig. 1B). Left ventricular end-diastolic diameter (LVEDD), left ventricular end-systolic diameter (LVESD), and end diastolic anterior wall thickness at the level of the papillary muscles were measured for at least three consecutive cardiac cycles, following the American Society for Echocardiology leading-edge method. Fractional shortening (FS) and ejection fraction (EF) were calculated as parameters of systolic function, as follows:

$$FS\ (\%) = (LVEDD - LVESD)/LVEDD$$

$$EF\ (\%) = [(LVEDD^3 - LVESD^3)/LVEDD^3].^4$$

Cardiac catheterization

To assess systolic and diastolic cardiac function, cardiac catheterization was performed under general anesthesia using 1% isoflurane, 8 weeks after the treatment procedure. A MicroTip catheter transducer (SPR-671; Millar Instruments, Inc.) and conductance catheters (Unique Medical

Co.) were placed longitudinally in the left ventricle (LV) from the apex and connected to an Integral 3-signal conditioner-processor (Unique Medical Co.). End-systolic pressure-volume relationships (ESPVR) were determined by transiently compressing the inferior vena cava. Data were recorded as a series of pressure–volume loops (~20), which were analyzed using Integral 3 software (Unique Medical Co.). The maximal and minimal rates of change in LV pressure (dP/dt max and dP/dt min, respectively) were obtained from steady-state beats using custom-made software. We assessed the early active part of the relaxation using the relaxation time constant (τ), which was determined from the LV pressure decay curve. After the hemodynamic assessment, the heart was removed for further biochemical and histological analyses.

Real-time quantitative PCR

Total RNA was extracted from cultured cell sheets or cardiac muscle tissue 8 weeks post-transplantation using TRIzol reagent (Invitrogen) and reverse transcribed into cDNA using TaqMan Reverse Transcription Reagents (Applied Biosystems). Subsequently, real-time PCR assays were performed using an ABI PRISM 7700 machine.[4,7,8] Hepatocyte growth factor (HGF), vascular endothelial growth factor (VEGF), basic fibroblast growth factor (bFGF), insulin growth factor (IGF), and thymosin β were assayed using rat-specific primers and probes (Applied Biosystems). The average copy number of gene transcripts for each sample was normalized to that for GAPDH.

Survival of grafted donor cells

The presence of grafted male cells in the female heart was quantitatively assessed by real-time PCR for the Y chromosome-specific gene *sry*. Four weeks after cell-sheet transplantation, genomic DNA was extracted from the entire LV walls using the QIAmp genomic DNA purification system (Qiagen). The signals for the autosomal single-copy gene were normalized to the amount of total DNA.[7] The primers were *sry*: forward, 5′ GCCTCAGGACATATTAATCTCTGGAG-3′; reverse, 5′-GCTGATCTCTGAATTCTGCATGC-3′.

Protein analysis

Enzyme-linked immunosorbent assay (ELISA) kits were used to measure proteins, such as HGF (Institute of Immunology) and VEGF (Quantikine; R&D) of rat origin, secreted from the cultured cell sheets *in vitro*, according to the manufacturers' suggested protocols. Values were calibrated for the extracted total proteins ($n=5$ in each group). The ELISA kits were also used to quantitatively analyze HGF (r-HGF) and VEGF (r-VEGF) of rat origin in heart tissue lysates ($n=5$ in each group).

Cytokine/chemokine multiplex immunology assay

The amount of each protein secreted from the cultured cell sheets *in vitro* was measured by Milliplex Rat Cytokine/Chemokine Panel Premixed 32Plex (Millipore), according to the manufacturer's instructions.[4] In this procedure, we applied human SMBs (h-SMBs) isolated and cultured from the patient (age 53 years, male) and expand *in vitro* as described previously.[6]

Histological analyses

Eight weeks after cell-sheet implantation, the hearts were dissected, fixed in 4% paraformaldehyde, and embedded in either optimum cutting temperature compound for 5-μm-thick cryosections or paraffin for 5-μm-thick sections ($n=5$ in each group) (Fig. 1). The paraffin-embedded sections were used for routine hematoxylin–eosin (HE) staining to assess the myocardial structure. Masson's trichrome staining was performed to assess cardiac fibrosis in the remote myocardium. The fibrotic cardiac area was calculated as the percentage of myocardial area. The data were collected from 10 individual views per heart at a magnification of ×200. The heart sections were also stained with an antibody to von Willebrand Factor (vWF) to assess capillary density, which was calculated as the number of positively stained capillary vessels that were 5–10 μm in diameter in 10 randomly selected fields in the peri-infarct area, per heart. To determine the extent of apoptosis, sections from frozen tissue samples were subjected to terminal deoxynucleotidyl transferase-mediated dUTP nick end labeling (TUNEL) with an *in situ* apoptosis detection kit (Apoptag; Chemicon). Image J software was used for quantitative morphometric analysis.

To detect r-SMBs, we used GFP transgenic Lewis rats.[15] Cryosections were stained with an anti-HGF antibody (1:50 dilution; LifeSpan BioSciences). To detect h-MSCs and differentiation of the transplanted cell sheet, sections were stained with an antibody to human leukocyte antigen (1:50 dilution; Dako). The secondary antibody was Alexa Fluor 555 goat anti-mouse (1:200 dilution; Molecular Probes). Cell nuclei were counterstained with 6-diamidino-2-phenylindole (DAPI; Invitrogen). The images were examined by fluorescence microscopy (Keyence).

Western blotting

Tissue homogenates from LV samples in the cell-sheet transplanted site ($n=3$ in each group, on day 1) were prepared using lysis buffer (100 mM Tris pH 7.4, 20% SDS, 10 mM EDTA. 10 mM NaF, 2 mM sodium orthovanadate). The equivalent total protein was loaded onto SDS-polyacrylamide gel electrophoresis gels. Antibodies obtained from Cell Signaling were antiphosphorylated STAT3 (#9145), antiphosphorylated Akt (#4051), anti-Bcl_2 (#2876), and anti-poly (ADP-ribose) polymerase (PARP) (#9542). The labeled membrane was stripped and then re-probed with anti-STAT3 (#9132), anti-AKT (#9272), and anti-cleaved PARP (#9545) antibodies. Blots were scanned, and quantitative analysis was performed using Image J software. The relative proportion of the phosphorylated STAT3 was referred to that of the STAT3. The relative proportion of the phosphorylated Akt was referred to that of the Akt. The relative proportion of the PARP, cleaved PARP, Bcl_2 was referred to that of the control group.

Statistical analysis

Continuous variables are expressed as the mean ± SD. The significance of differences was determined using a two-tailed multiple *t*-test with Bonferroni correction following repeated-measures analysis of variance for individual differences. A *p*-value less than 0.05 was considered to be statistically significant. All statistical calculations were performed using the SPSS software (version 11.0; SPSS, Inc.).

Results

Production and release of cytokines/chemokines by cell sheets

Both h-SMBs and h-MSCs, as analyzed by cytokine antibody array, released abundant angiogenic factors *in vitro*, with distance profiles (Fig. 2A). Co-cultures of h-SMBs and h-MSCs showed significantly enhanced levels of HGF, VEGF, Leptin, and PECAM-1, but not of follistatin, G-CSF, IL-8, or PDGF-BB from the h-SMBs.

The seeding ratio of 4:1 r-SMBs:h-MSCs elicited the greatest *in vitro* mRNA expression of rat HGF and VEGF by real-time PCR (Fig. 2B). The mRNA levels of SMB-derived r-HGF and r-VEGF, analyzed by real-time PCR using rat-specific primers, were significantly greater in the co-cultured cell sheets than r-SMB-only ones (Fig. 2C), whereas the mRNA levels of IGF-1, bFGF, SDF-1, and TMSB4 were essentially the same (Supplementary Fig. S1; Supplementary Data are available online at www.liebertpub.com/tea). No mRNAs for cytokines of rat origin were detected in h-MSC-only cell sheets. Rat HGF and VEGF in the culture supernatants, analyzed by ELISA with rat-specific primary antibodies, were significantly higher in the co-culture supernatants than the r-SMB-only ones, and no rat cytokines were detected in the h-MSC-only supernatants (Fig. 2D).

Cardiac functional recovery after cell-sheet transplantation

The effects of cell-sheet transplantation on cardiac function were assessed in a rat chronic ischemic heart-failure model. Two weeks after permanent occlusion of the LCA, the LV developed echocardiographic features typical of chronic ischemic heart failure, including decreased FS, EF, and anterior wall thickness, and increased end-diastolic and systolic diameter (EDD and ESD, respectively). Following myocardial

A Cytokine/Chemokine multiplex immunology assay

	SMB+MSC	SMB	MSC	Medium only
Follistatin (pg/ml)	276±35*,†	350±56*	127±8.0	3.3
G-CSF (pg/ml)	333±44*,†	487±89*	7.7±0.7	1
HGF (pg/ml)	1190±256*,†	167±28*	695±44	3.8
IL-8 (pg/ml)	805±36*,†	1079±138*	579±29	0.6
Leptin (pg/ml)	1335±690*,†	262±40	195±13	59
PDGF-BB (pg/ml)	51±11*	25±2*	51±3	3.3
PECAM-1 (pg/ml)	438±70*	239±71*	386±16	64
VEGF (pg/ml)	5673±812*,†	1402±272	2019±184	1.9

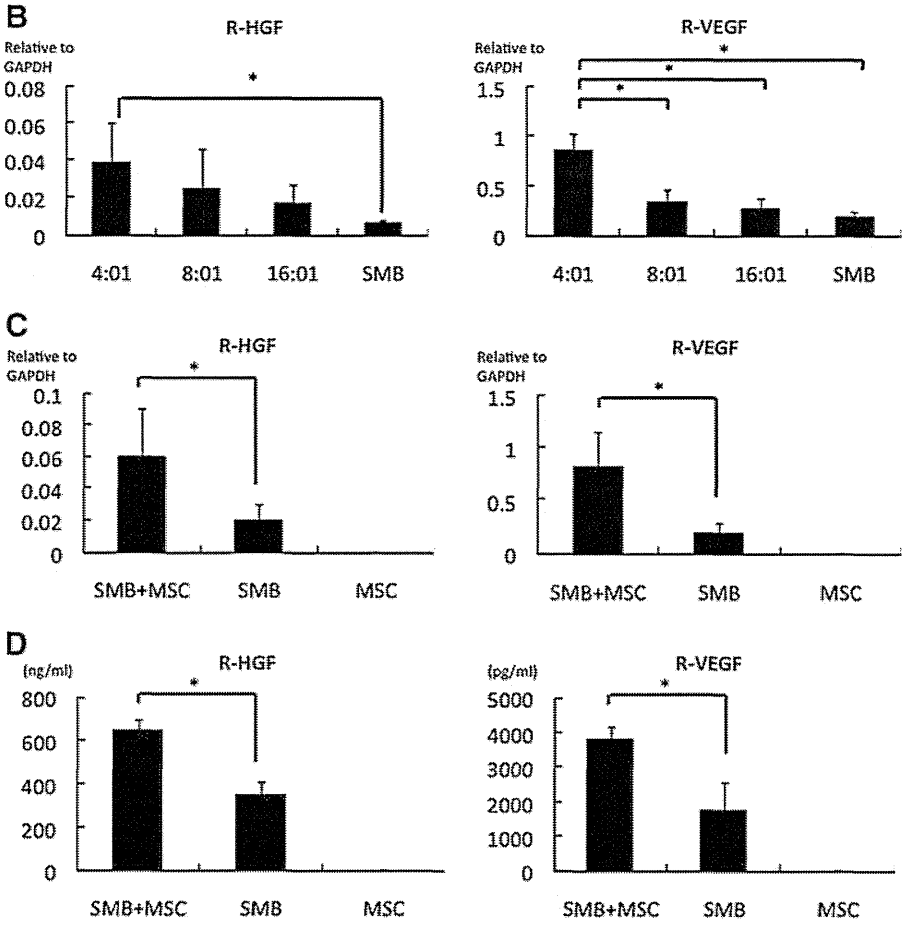

FIG. 2. Production and release of angiogenic factors by cell sheets. **(A)** Cytokine/chemokine multiplex immunology assay results from cultured cell sheets *in vitro*, prepared from human SMBs, human MSCs (h-MSCs), or both. SMB+MSC showed significantly enhanced the release of HGF, VEGF, leptin, and PECAM-1. $N=4$ in each group. $^{*}p<0.05$ versus SMB. $^{\dagger}p<0.05$ versus MSC. **(B)** Optimal seeding ratio of rat SMBs (r-SMBs) to h-MSCs. The *in vitro* mRNA levels of rat HGF and VEGF, analyzed by real-time PCR, were highest at 4:1 r-SMBs:h-MSCs. $N=4$ in each group. $^{*}p<0.05$. **(C)** mRNA levels in cultured cell sheets determined by real-time PCR using rat-specific primers. The SMB+MSC sheets expressed significantly more HGF and VEGF than the SMB-only ones. $N=5$ in each group. $^{*}p<0.05$. **(D)** Secretion of cytokines into the culture medium determined by enzyme-linked immunosorbent assay (ELISA) kits. The SMB+MSC sheets secreted significantly more HGF and VEGF than the SMB-only sheets. $N=5$ in each group. $^{*}p<0.05$. G-CSF, granulocyte-colony stimulating factor; HGF, hepatocyte growth factor; IL, interleukin; PDGF, platelet-derived growth factor; PECAM, platelet/endothelial cell adhesion molecule; VEGF, vascular endothelial growth factor. Error bars=SD.

infarction (MI), FS, EF, and anterior wall thickness showed steady reductions, whereas EDD/ESD showed steady increases, suggesting progressive LV remodeling.

Following either SMB-only or MSC-only cell-sheet transplantation, the heart showed mild recovery, including increases in FS, EF, and anterior wall thickness. At 2, 4, 6, and 8 weeks after treatment, FS, EF, and anterior wall thickness were significantly greater following SMB-only or MSC-only cell-sheet transplantation than the control, and significantly better recovery was obtained using the co-cultured cell sheets than either single cell-type sheet (Fig. 3A).

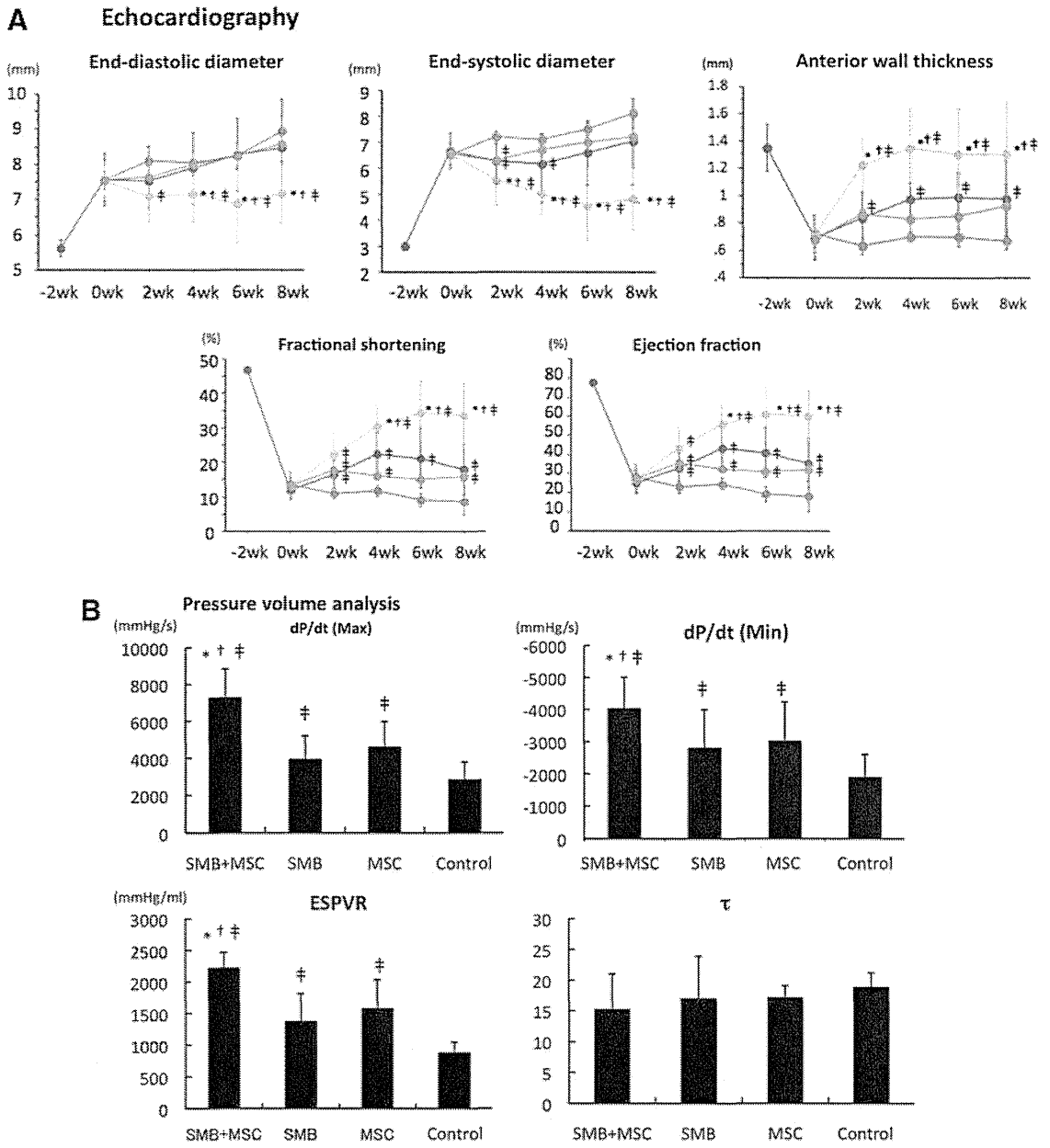

FIG. 3. Cardiac functional recovery after cell-sheet transplantation. **(A)** Echocardiographic analysis. Fractional shortening, ejection fraction, and anterior wall thickness were significantly improved 2, 4, 6, and 8 weeks after cell-sheet transplantation in the SMB+MSC sheet group, compared with the other three groups. Left ventricular end-diastolic and end-systolic diameters in the SMB+MSC sheet group were significantly decreased 4, 6, and 8 weeks after cell-sheet transplantation, compared with the other three groups ($N=10$ in each group. SMB+MSC group, green line; SMB group, blue line; MSC group, pink line; control group, red line). **(B)** Hemodynamic measurements determined by cardiac catheterization ($n=10$ in each group). Max. and min. dP/dt and ESPVR significantly improved in the SMB+MSC group, compared with the other three groups. Max. dP/dt, maximal rate of change in left ventricular pressure; min. dP/dt, minimal rate of change in left ventricular pressure; ESPVR, end-systolic pressure-volume relationship; EDPVR, end-diastolic pressure-volume relationship; τ, active part of relaxation shown by the relaxation time constant. $N=10$ in each group. $^{*}p<0.05$ versus SMB-only cell sheet. $^{\dagger}p<0.05$ versus MSC-only cell sheet. $^{\ddagger}p<0.05$ versus control. n.s., not significant. Error bars=SD. Color images available online at www.liebertpub.com/tea

Assessment by LV catheter showed a similar trend. Eight weeks after transplantation, the maximal and minimal rate of change in LV pressure (max. dP/dt and min. dP/dt, respectively) and end-systolic pressure-volume relationship (ESPVR) were significantly greater following either single-cell-type cell-sheet transplantation than the control, but τ was significantly different. After the co-culture cell-sheet transplantation, the max. dP/dt, min. dP/dt, and ESPVR improved further, with no significant difference in EDPVR or τ (Fig. 3B).

Reverse remodeling after co-culture cell-sheet transplantation

The LV structure was better maintained after SMB-only or MSC-only cell-sheet transplantation, compared to the control, in which the LV cavity was severely enlarged with a thin anterior wall, as assessed by HE staining (Fig. 4A). The LV structure was even better maintained after the co-culture cell-sheet transplantation. In the control, abundant collagen accumulations were observed in the infarct area, and diffuse fibrotic changes were induced in the remote area, whereas collagen accumulation was attenuated in both the remote area with the single cell-type sheet transplants, as assessed by Masson's trichrome staining (Fig. 4B, C). Fibrotic changes in the remote area were further attenuated by transplantation of the co-cultured cell sheet (Fig. 4D).

A greater number of vWF-positive blood vessels was detected in the peri-infarcted myocardium following the transplantation of either single-cell-type cell sheet, compared to the control (Fig. 5A), and even more vWF-positive blood vessels were seen with transplantation of the co-cultured cell sheet. The capillary density in the peri-infarcted myocardium, which was semi-quantitatively assessed in 10 randomly selected individual fields, was significantly greater following the transplantation of either single-cell-type cell sheet, compared to the control (Fig. 5B), and it was further increased after the co-cultured cell-sheet transplantation.

Major intercellular signaling molecules relevant to angiogenesis and cell survival were analyzed by western blotting. The ratio of p-STAT3 over total STAT3 was greatly increased after co-cultured cell-sheet transplantation (Fig. 5C).

Survival of transplanted cells in the heart

Four weeks after the cell-sheet transplantation, significantly more transplanted rat cells survived in co-cultured sheets than SMB-only sheets, as analyzed by PCR assays for the Y-chromosome-specific *Sry* gene (Fig. 6A).

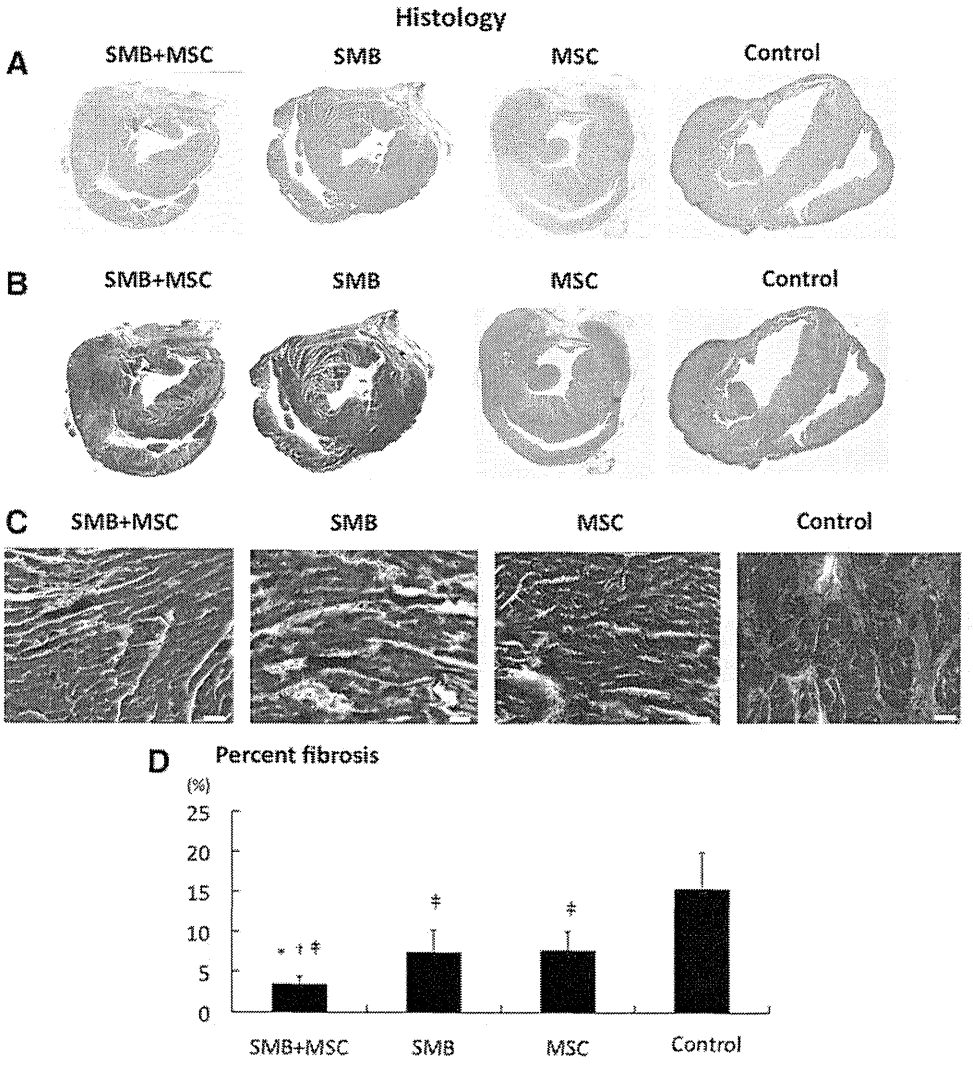

FIG. 4. Histological reverse remodeling after cell-sheet transplantation. **(A)** Macroscopic (×40) views of the heart stained by hematoxylin–eosin. **(B)** Macroscopic (×40) views of the heart stained by Masson's trichrome. **(C)** Microscopic (×200) representative Masson's trichrome staining at the remote myocardium (white bar = 40 μm). **(D)** Quantification of percent fibrosis at the remote area. Significant suppression of fibrosis was found after SMB + MSC sheet transplantation compared with the other three groups. $N = 5$ in each group. $^{*}p < 0.05$ versus SMB. $^{\dagger}p < 0.05$ versus MSC. $^{\ddagger}p < 0.05$ versus control. Error bars = SD. Color images available online at www.liebertpub.com/tea

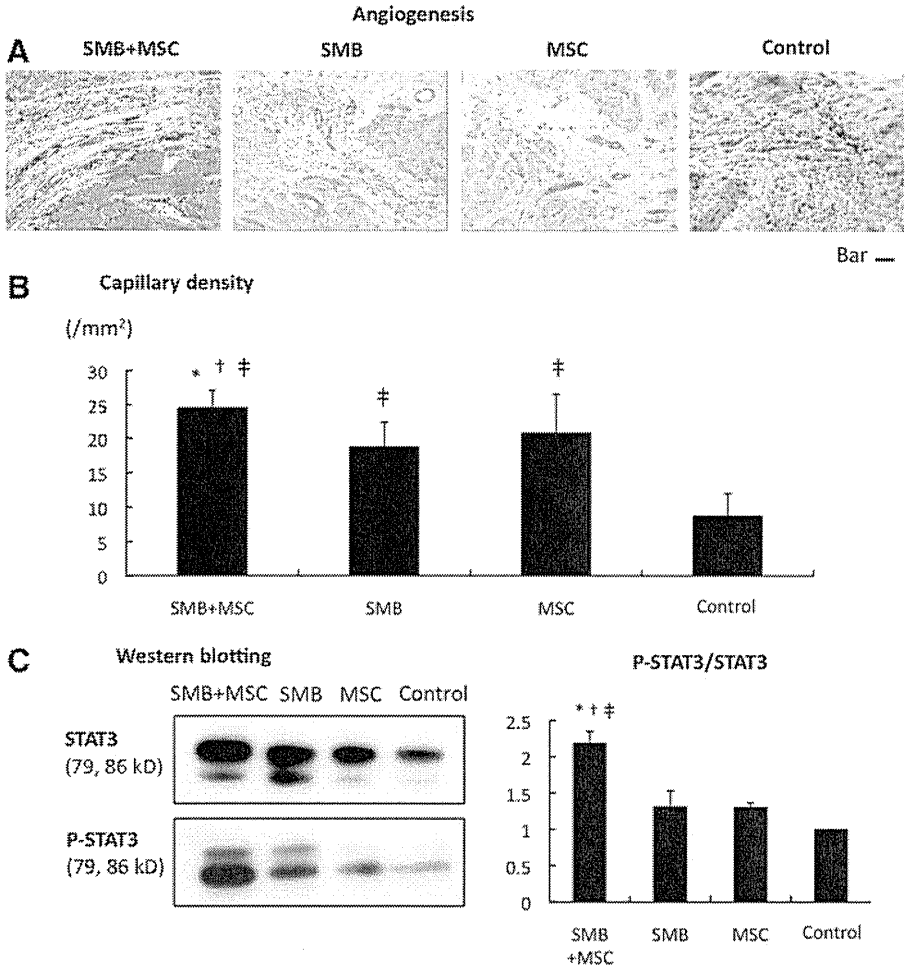

FIG. 5. Angiogenesis. **(A)** Microscopic (×100) views of sections of the peri-infarct border-zone region stained with anti-von Willebrand factor antibody (factor VIII) in the four groups (bar = 50 μm). **(B)** Capillary density: the SMB + MSC group showed significant improvement in capillary density as assessed by immunostaining for von-Willebrand factor-positive blood vessels. $N = 5$ in each group. **(C)** Western blotting showing enhanced STAT3 phosphorylation over total STAT3 in the SMB + MSC sheet group. $N = 3$ in each group. $^{*}p < 0.05$ versus SMB. $^{\dagger}p < 0.05$ versus MSC. $^{\ddagger}p < 0.05$ versus control. Error bars = SD. STAT3, signal transducer and activator of transcription 3. Color images available online at www.liebertpub.com/tea

The percentage of TUNEL-positive myocytes was significantly lower following the transplantation of the co-cultured cell sheet compared to the control (Fig. 6B).

Akt-1 and Bcl-2 were highly expressed in the heart following transplantation of the SMB-only or co-cultured cell sheet, compared with the control, as analyzed by real-time quantitative PCR using rat-specific primers (Fig. 6C).

Notably, among apoptosis-signaling molecules, Bcl_2 and cleaved PARP were increased 1 day after the co-culture cell-sheet transplantation. There was no significant difference in the ratio of phosphorylation of Akt over Akt (Fig. 6D).

Upregulation of cardioprotective factors in the myocardium after cell-sheet transplantation

The mRNA expression of cardioprotective factors, such as HGF, VEGF, IGF-1, and bFGF, in the infarct and infarct-remote areas of the myocardium was analyzed by real-time PCR using rat-specific primers, which detected factors released by transplanted SMB or the native myocardium. The expression of these factors was not significantly different after transplantation of either single-cell-type cell sheet or no treatment, except for HGF expression in the infarct area, which was significantly greater after the SMB-only sheet transplantation (Fig. 7A, B). In contrast, following transplantation of the co-cultured cell sheet, the HGF and VEGF levels in the infarct area were significantly greater than after transplantation of either single cell-type cell sheet or control, although the levels of IGF-1 and bFGF were unchanged (Fig. 2A). The intramyocardial protein levels of HGF and VEGF, analyzed by ELISA, were significantly greater after transplantation of the co-cultured cell sheet than of either single-cell-type cell sheet or no treatment (Fig. 7C).

Immunoconfocal microscopy showed that HGF was found in the transplanted SMBs from the co-cultured cell sheet (Fig. 8A).

MSCs differentiate into new vessels in situ

The differentiation capacity of the transplanted h-MSCs was assessed by immunoconfocal microscopy. As expected, no human-derived cells were seen in either the r-SMB-only transplantation group or the control group. However, human vWF-positive staining was observed in the host vessels in both the co-cultured cell-sheet group and the h-MSC-only cell-sheet transplantation group. Thus, the h-MSCs could differentiate into vessel walls *in vivo* (Fig. 8B).

Discussion

Here, we demonstrated that SMB cell sheets abundantly synthesized and extracellularly released multiple cytokines and chemokines, and adding MSCs enhanced the SMB cell